7750–7763 *Nucleic Acids Research, 2011, Vol. 39, No. 17* *Published online 11 June 2011*
doi:10.1093/nar/gkr470

PDE12 removes mitochondrial RNA poly(A) tails and controls translation in human mitochondria

Joanna Rorbach, Thomas J. J. Nicholls and Michal Minczuk*

MRC Mitochondrial Biology Unit, Wellcome Trust/MRC Building, Hills Road, Cambridge CB2 0XY, UK

Received March 31, 2011; Revised May 20, 2011; Accepted May 21, 2011

ABSTRACT

Polyadenylation of mRNA in human mitochondria is crucial for gene expression and perturbation of poly(A) tail length has been linked to a human neurodegenerative disease. Here we show that 2′-phosphodiesterase (2′-PDE), (hereafter PDE12), is a mitochondrial protein that specifically removes poly(A) extensions from mitochondrial mRNAs both *in vitro* and in mitochondria of cultured cells. In eukaryotes, poly(A) tails generally stabilize mature mRNAs, whereas in bacteria they increase mRNA turnover. In human mitochondria, the effects of increased PDE12 expression were transcript dependent. An excess of PDE12 led to an increase in the level of three mt-mRNAs (ND1, ND2 and CytB) and two (CO1 and CO2) were less abundant than in mitochondria of control cells and there was no appreciable effect on the steady-state level of the remainder of the mitochondrial transcripts. The alterations in poly(A) tail length accompanying elevated PDE12 expression were associated with severe inhibition of mitochondrial protein synthesis, and consequently respiratory incompetence. Therefore, we propose that mRNA poly(A) tails are important in regulating protein synthesis in human mitochondria, as it is the case for nuclear-encoded eukaryotic mRNA.

INTRODUCTION

Mitochondria are vital organelles as they provide energy to the cell via the process of oxidative phosphorylation (OXPHOS). The 16.6 kb circular human mitochondrial genome (mtDNA) encodes 2 rRNAs, 22 tRNAs and 13 essential protein components of the OXPHOS complexes (1). The remaining proteins of the mitochondrial proteome (>99%), including all factors necessary for the maintenance and expression of mtDNA, are encoded by the nucleus. Both mtDNA strands (termed H and L) are almost entirely transcribed from the promoters located in the control non-coding region. Resulting polycistronic RNA molecules are then processed to produce mRNAs, rRNAs and tRNAs (2). Human mitochondrial mRNAs (mt-mRNAs) released by this processing do not contain introns and lack any cap or modification at the 5′-end; however, they do have ~50 adenosine residues added at the 3′-terminus by a dedicated mitochondrial poly(A) polymerase (3,4). Seven of the 13 open reading frames (ORFs) require polyadenylation to create a translation stop codon (5).

Regulation of human mitochondrial RNA (mt-RNA) surveillance and turnover has not been well characterized thus far (6,7); also the regulatory mechanisms that control mitochondrial translation are poorly understood (8). In many systems, RNA polyadenylation plays an important role both in controlling mRNA stability and in modulating translation (9). The human mitochondrial poly(A) polymerase (hmtPAP) responsible for the synthesis of the mitochondrial poly(A) extensions has been identified (3,4), however, inactivation of this enzyme did not yield a clear answer to the role of poly(A) extensions in the stability of mt-RNAs. The siRNA-mediated knockdown of hmtPAP led to shortening of mitochondrial 3′-poly(A) extensions, but this either did not affect the stability (3) or resulted in decreased steady-state levels of some mt-mRNAs (4,10). Furthermore, analysis of the ATP6/8 mt-mRNA (RNA14) harbouring a microdeletion in the translation stop codon in a patient-derived cell line showed that this message has shortened poly(A) tails and is less stable, consistent with the poly(A) tail stabilizing the ATP6/8 mRNA (11). Another approach based upon mitochondrial targeting of a poly(A)-specific 3′-exoribonuclease PARN led to efficient RNA deadenylation; however, this had a variable effect on mt-mRNA steady-state levels, increasing or decreasing particular mRNAs with no effect on others (12). Another previous study showed that a fraction of the mt-RNA is truncated and internally polyadenylated, consistent with the possibility that a poly(A)-dependent degradation pathway exists in human mitochondria (13). Also, oligoadenylation at the 3′-termini has been suggested to precede the addition of long poly(A) tails, (14,15), but to date no enzyme responsible for the

*To whom correspondence should be addressed. Tel: +0044 1223 252750; Fax: +0044 1223 252755; Email: michal.minczuk@mrc-mbu.cam.ac.uk

synthesis of oligo(A) extensions has been identified. By analogy with the role of RNA polyadenylation in the cytosol of eukaryotes, poly(A) tails may also play a role in modulating mitochondrial translation. However, this potential function has received very little attention thus far (12).

Deadenylase enzymes ensure changes of the lengths of mRNA poly(A) in order to regulate mRNA stability and therefore protein production. All known human deadenylases belong to two enzyme families classified on the basis of conserved nuclease motifs (16): (i) the DEDD family, e.g. POP2, PARN and PAN2 deadenylases and (ii) the ribonucleases of the exonuclease/endonuclease/phosphatase (EEP) family, e.g. CCR4 (CNOT6), Nocturnin and ANGEL (16). All human deadenylases characterized thus far have been localized either to the cytosol or the nucleus (or found to shuttle between these two compartments). Therefore, the mechanism of regulation of mRNA poly(A) tail length in mitochondria was not known.

We studied PDE12 because it shares sequence homology with known RNA deadenylases and *in silico* analysis predicted its a mitochondrial localization. PDE12 is an exoribonuclease with a preference for homo-adenine oligonucleotides, and removes poly(A) tail extensions from mt-mRNAs *in vitro* and in mitochondria of cells in culture. Deadenylation altered the steady-state level of some, but not other, mitochondrial mRNAs, which may explain earlier contradictory results of the effect of mitochondrial poly(A) tails on controlling mt-mRNA stability. We also show that deadenylation of mt-mRNA led to a marked inhibition of mitochondrial protein synthesis, suggesting that poly(A) tails modulate translation in mitochondria.

MATERIALS AND METHODS

Plasmids

In order to construct the pcDNA5-PDE12.Strep2.Flag plasmid used to generate an inducible Flp-In T-Rex^{TM} human embryonic kidney 293 T (HEK293T) cell line, two oligonucleotides encoding an AgeI restriction site, Flag and Strep2 epitope tags were annealed and cloned into XbaI (5′) and ApaI (3′) restriction sites of pcDNA5/FRT/TO (Invitrogen). The resulting plasmid was named pcDNA5-FST2. The cDNA-encoding PDE12 (IMAGE clone: 4823249) was then modified by PCR to introduce unique KpnI (5′) and AgeI (3′) sites and the resulting fragment was cloned into pcDNA5-FST2 using the above restriction sites. The E351A catalytic mutant was generated using PCR-based mutagenesis and the resulting cDNA was cloned into pcDNA5-FST2 as above. For transfection of mammalian cells plasmid, DNA was purified using a Qiafilter MidiPrep Kit (Qiagen).

Maintenance, transfection and growth analysis of mammalian cell lines

Human 143B osteosarcoma (HOS) cells that are routinely used by us for immunofluorescence localization of mitochondrial proteins were cultured in Dulbecco's Modified Eagle Medium (DMEM) containing 2 mM L-glutamine (Invitrogen) with 10% FBS (PAA Laboratories). For immunofluorescence experiments, HOS cells were electroporated with pcDNA5-PDE12.Strep2.Flag using Cell Line Nucleofector (Lonza) and buffer kit V (Lonza) applying programme I-13.

The Flp-In T-Rex^{TM} HEK293T cell line (Invitrogen), which allows for the generation of stable, doxycycline-inducible expression of transgenes by FLP recombinase-mediated integration was used to express PDE12 .Strep2.Flag and the E351A catalytic mutant. HEK293T cells were grown in DMEM containing 2 mM L-glutamine (Invitrogen), 10% tetracycline free FCS (Autogen Bioclear) and supplemented with 100 μg/ml Zeocin (Invivogen) and 15 μg/ml Blasticidin (Invivogen). Twenty-four hours prior to transfection cells were split to 10 cm plates, grown to 80–90% confluence and transfected using Cell Line Nucleofector (Lonza), buffer kit V (Lonza) applying programme A-23. Twenty-four hours after transfection, the selective antibiotics hygromycin (100 μg/ml, Invivogen) and blasticidin (15 μg/ml) were added and the selective medium was replaced every 3–4 days. For growth on respiratory substrates, the medium contained glucose-free DMEM (Gibco), 0.9 mg/ml galactose, 1 mM sodium pyruvate, 10% (v/v) FCS and 2 mM L-glutamine.

For growth measurements cells were plated in six-well plates and grown with 50 ng/ml of doxycycline in galactose or glucose containing medium. Cells were harvested from replicate plates on alternate days and total cell counts made using a Neubauer haemocytometer.

Immunodetection of proteins

The immunofluorescence localization of proteins in fixed HOS cells were performed as described previously (17). The following antibodies were used: anti-Flag IgG (Sigma, 1:200), FITC-conjugated anti-mouse IgG (Sigma, 1:200). Immunofluorescence images were captured using a Zeiss LSM 510 META confocal microscope.

For immunoblot analysis, equal amounts of proteins corresponding to total cell lysates or protein fractions were subjected to SDS–PAGE, semi-dry transferred to nitrocellulose membranes, blocked in 5% non-fat milk (Marvel) in PBS for 1 h and incubated with specific primary antibodies in 5% non-fat milk in PBS for 1 h or overnight. The blots were further incubated with HRP-conjugated secondary antibodies in 5% non-fat milk in PBS for 1 h and visualized using ECL^{+} (Amersham).

The primary antibodies used were: rabbit anti-PDE12 (Abcam, 1:1000), mouse anti-FLAG IgG (Sigma, 1:5000), rabbit anti-β-actin IgG (1:7000, Sigma), mouse anti-CO2 IgG (1:5000, Abcam), rabbit anti-TFAM IgG (kindly donated by Professor Rudolf Wiesner, University of Cologne, 1:4000), mouse anti-GAPDH IgG (Abcam, 1:10 000), mouse anti-Complex I subunit NDUFB8 (MitoSciences, 1:2000), mouse anti-Complex II subunit 30 kDa (MitoSciences, 1:2000), mouse anti-Complex III subunit Core 2 (MitoSciences, 1:2000), rabbit anti-VDAC-1 IgG (Abcam, 1:5000), mouse anti-DAP3 IgG (Abcam, 1:1000) and goat anti-MRPL3 (Abcam, 1:1000).

Secondary antibodies were: anti-rabbit IgG-HRP (Promega, 1:2000), anti-mouse IgG-HRP (Promega, 1:2000) and anti-goat IgG-HRP (Sigma, 1:1000).

Protein purification

Mitochondria derived from HEK293T cells expressing PDE12.Strep2.Flag or the E351A catalytic mutant were isolated as described previously (18) and resuspended to 8 mg protein/ml in 40 mM HEPES (pH 7.6), 10 mM EDTA, 4 mM DTT, 0.4 mM PMSF, 300 mM NaCl and protease inhibitor cocktail (Roche). Next, the mitochondria were lysed by mixing with an equal volume of 0.8% dodecylmaltoside (DDM) in water, on a roller at 4°C for 30 min. The lysate was centrifuged at 1600 g_{max} for 10 min to remove insoluble debris and the supernatant was loaded onto a gravity flow Strep-Tactin column (IBA) and the flow-through re-loaded twice. The column was washed sequentially with five column volumes (CV) of washing buffer containing 20 mM HEPES (pH 7.6), 1 mM EDTA, 2 mM DTT, 0.2 mM PMSF, 150 mM NaCl, 0.05% DDM, protease inhibitors (Roche) and eluted six times with 0.5 CV elution buffer (washing buffer plus 10 mM desthiobiotin). Peak fractions containing PDE12.Strep2.Flag were concentrated using Vivaspin 2 Centrifugal Concentrators (Sartorius stedim), supplemented with glycerol to 20% and stored at −80°C. In order to assess the purity and identity of the Strep-Tactin purified proteins, the preparations were separated by SDS–PAGE, Coomassie stained and protein bands were excised from gels and identified by mass spectrometry.

Nuclease assays

The reaction substrates were prepared by: (i) 5′-end-labelling of RNA or DNA oligonucleotides with T4 Polynucleotide Kinase (New England Biolabs) according to the manufacturer's instructions; (ii) *in vitro* run off transcription of PCR-generated templates [encompassing T7 promoter (5′) and 50 adenine nucleotides where appropriate (3′)] using MAXIscript® T7 Kit (Ambion) in the presence of 0.825 μM α-^{32}P UTP (3000 Ci/mmol, Perkin Elmer] according to the manufacturer's instructions; or (iii) ligating the 3′-end of RNA oligonuclotides with radioactive pCp (PerkinElmer) using T4 RNA ligase (New England Biolabs).

The reaction mixture of 20 μl containing 5 pmoles of the substrate, 50 mM HEPES (pH 8.0), 10 mM $MgCl_2$, 0.5 mM DTT, 100 μg/ml BSA, 4 U of RNasin (Promega) and 8.5 pmols of PDE12 or E351A catalytic mutant were incubated at 37°C for the indicated time. The samples were analysed on 5–10% urea polyacrylamide gels in 1× glycerol tolerant buffer (GTB) containing 90 mM Tris–base, 30 mM Taurine and 0.5 mM EDTA.

Analysis of mitochondrial poly(A) by circular reverse transcription–PCR assay

Circular reverse transcription PCR (cRT–PCR) labelling and sequencing were used to determine both 5′- and 3′-ends of mt-RNA as described in Tomecki *et al.* (3) with minor modifications. Briefly, 2.5 μg of total RNA was circularized with T4 RNA ligase (New England Biolabs) in the presence of DNAse I (Roche) followed by phenol–chloroform extraction and ethanol precipitation. Reverse transcription was carried out using Omniscript Reverse Transcriptase (Qiagen) with a gene-specific reverse primer, generally termed R1. Newly synthesized cDNA was used as a template for a PCR reaction, primed with R1 primer and a forward primer, F1. The region amplified contained the junction of the 5′- and 3′-extremities. A second round of PCR with the nested reverse primer, R2, and forward primer, F2, was applied. Products were cloned into pCR®II-TOPO vector (TOPO TA Cloning Kit, Invitrogen) and sequenced.

For CO2 analysis the following primers were used:

F1: GGTATACTACGGTCAATG,
R1: GTTCAGACGGTTTCTATTTC,
F2: TATAGCACCCCCTCTACCCC,
R2: GTAGACCTACTTGCGCTGCAT and
F2: TATAGCACCCCCTCTACCCC.

ND1 analysis:

F1: TAAACACCCTCACCACTACA,
R1: GCCTAGAATTTTTCGTTCGG,
F2: TACAATCTCCAGCATTCCC and
R2: AGGAGTAGGAGGTTGGCCAT.

RNA isolation and northern blotting

Total RNA from HEK293T cells was isolated using Trizol (Invitrogen) according to the manufacturer's instructions. For northern blots, RNA was resolved on 1% agarose gels containing 0.7 M formaldehyde in 1× MOPS buffer, transferred to a nylon membrane in 2× SSC and hybridized with radioactively labelled PCR fragments corresponding to appropriate regions of mtDNA.

Measurement of mitochondrial respiration and membrane potential

HEK293T cells expressing PDE12 were seeded at 3×10^4 cells/well in 200 μl growth medium in XF 24-well cell culture microplates (Seahorse Bioscience) and incubated at 37°C in 5% CO_2 for 36–40 h. One hour before the assay growth medium was removed and replaced with assay medium (low buffered DMEM, 10 mM L-glutamine, 1 mM sodium pyruvate, 2 mM glucose), with one rinse with assay medium, and left to stabilize in a 37°C non-CO_2 incubator. Analysis was performed in quadruplicates using XF24 Extracellular Flux Analyzer (Seahorse Bioscience). The wells containing cells were sequentially injected with 20 mM 2-deoxyglucose (2-DG) to inhibit glycolysis, 100 nM oligomycin to inhibit ATP synthase, 500–1000 nM carbonylcyanide-4-trifluorometho-xyphenylhydrazone (FCCP) to uncouple the respiratory chain and 200 nM rotenone to inhibit complex I. Oxygen consumption rate (OCR) was measured for each well every 5 min before and after each injection. Test compounds: 2-DG, oligomycin, FCCP and rotenone were obtained from Sigma.

For membrane potential measurements, 4×10^5 cells were stained with 100 nM tetramethylrhodamine ethyl ester (TMRE) (Invitrogen) in PBS for 1 h at 37°C, trypsinized, resuspended in PBS and analysed by BD LSRII flow cytometer. Debris and apoptotic cells were excluded from the analyses using Forward and Side Scatter gate. Acquired data were analysed by FlowJo software (Tree Star, Inc.). Experiments were performed for three independent transgene inductions with triplicate measurements based on 20 000 events.

^{35}S-methionine metabolic labelling of mitochondrial proteins

Stably transfected HEK293T cells expressing PDE12 (or E351A) were induced with doxycycline (50 ng/ml) for 2 or 4 days prior to ^{35}S labelling. Growth medium was replaced with methionine/cysteine-free DMEM (Sigma) supplemented with 2 mM L-glutamine, 48 μg/ml cysteine and 50 μg/ml uridine. The cells were incubated for 2×10 min in this medium and then transfered into fresh methionine/cysteine-free DMEM medium containing 10% (v/v) dialysed FCS and emetine dihydrochloride (100 μg/ml). Cells were incubated for 10 min before addition of 120 μCi/ml of [^{35}S]-methionine. Labelling was performed for 15 min and the cells were washed twice with standard growth medium. Protein samples (30 μg) were separated by 4–12% SDS–PAGE and products visualized and quantified with a PhosphorImager system with ImageQuant software (Molecular Dynamics, GE Healthcare).

Analysis of mitochondrial ribosome profile on density gradients

Total cell lysates (0.7 mg) were loaded on a linear sucrose gradient [2 ml 10–30% (v/v)] in 50 mM Tris–HCl (pH 7.2), 10 mM $Mg(OAc)_2$, 80 mM NH_4Cl, 0.1 M KCl, 1 mM PMSF and centrifuged for 2 h 15 min at 100 000 g_{max} at 4°C (39 000 rpm, Beckman Coulter TLS-55 rotor). Twenty fractions (100 μl) were collected and 10 μl aliquots were analysed directly by western blotting.

Other procedures

Other procedures including assessing mtDNA copy number by quantitative PCR and the ribonuclease protection assay (RPA) are described in Supplementary Data.

RESULTS

In silico characterization and mitochondrial localization of PDE12

The previously identified 2′-PDE protein (19), hereafter PDE12, contains the domain characteristics of the endonuclease/exonuclease/phosphatase (EEP) family of proteins (PFAM: PF03372). In order to examine the genetic divergence of human PDE12 and other human proteins with the PF03372 domain we built a classification tree (Figure 1A). The analysis revealed that human PDE12 belongs to a subgroup that contains all established and putative human deadenylases from the EEP family (Figure 1A, red) as described by Goldstrohm and Wickens (16). Human PDE12 shares the same general domain architecture (Figure 1B) and all key catalytic residues with other EEP deadenylases (Supplementary Figure S1). Furthermore, 3D homology modelling of the PDE12 active site based on the crystal structure of the poly(A)-specific ribonuclease CNOT6L (20) indicated a similar arrangement of the key catalytic residues (Figure 1C and D).

Several computer programmes that scan the N-terminal region of proteins for the presence of a putative mitochondrial targeting sequence (MTS) returned a high probability of a MTS in PDE12 (MultiLoc – 98.0%, MitoProt II – 94%, Predotar – 81%, TargetP – 77% and PSORT – 75%). Moreover, PDE12 is listed in the compendium of predicted mitochondrial proteins ['Mitocarta', (21)] constructed on the basis of subtractive proteomics of mitochondria from different tissues, mRNA co-expression, transcriptional induction during mitochondrial proliferation, homology studies and more. Therefore, PDE12 represented a strong candidate for a mitochondrial poly(A)-specific ribonuclease.

Indeed, while our manuscript was in preparation, Poulsen *et al*. (22) reported that a His-tagged version of PDE12 (2′-PDE) is localized in the mitochondrial matrix of HeLa cells (as shown by immunofluorescence, *in vitro* import of ^{35}S-labelled recombinant protein and mass spectrometry of mitochondrial fractions). Transiently expressed PDE12 with Flag and Strep2 tags also co-localizes with mitochondria, in HOS cells (Figure 2A), and endogenous PDE12 co-fractionates with the well-characterized mitochondrial matrix protein TFAM and the mitochondrial inner membrane CO2 (Figure 2B). Therefore, it is now established by two laboratories, using four different techniques, that the PDE12 protein is present inside the mitochondria of human cells.

PDE12 has deadenylase activity *in vitro*

Since PDE12 contains a domain similar to deadenylases (Figure 1), we tested PDE12 for sequence-specific nuclease activity. We generated a point mutation in a putative magnesium-binding residue by substituting glutamate at position 351 with alanine (E351A, Figure 1C, cyan). A point mutation in the analogous residue severely compromised the activity of other EEP deadenylases (20,23).

In order to purify the enzymes for biochemical studies, a Flag- and Strep2-tagged version of the PDE12 wild-type and the E351A mutant were introduced into HEK293T cells. The mitochondrial localization of the overexpressed wild-type PDE12 and the E351A mutant in HEK293T cells was confirmed by fractionation after induction of the transgenes for 48 h with 50 ng/ml of doxycycline. Both proteins were concentrated in the mitochondrial fraction (Supplementary Figure S2A). The enzymes were purified from mitochondria of HEK293T cells on a streptavidin-coated matrix (see 'Material and Methods' section). SDS–PAGE analysis demonstrated a substantial enrichment of the tagged proteins (Supplementary Figure

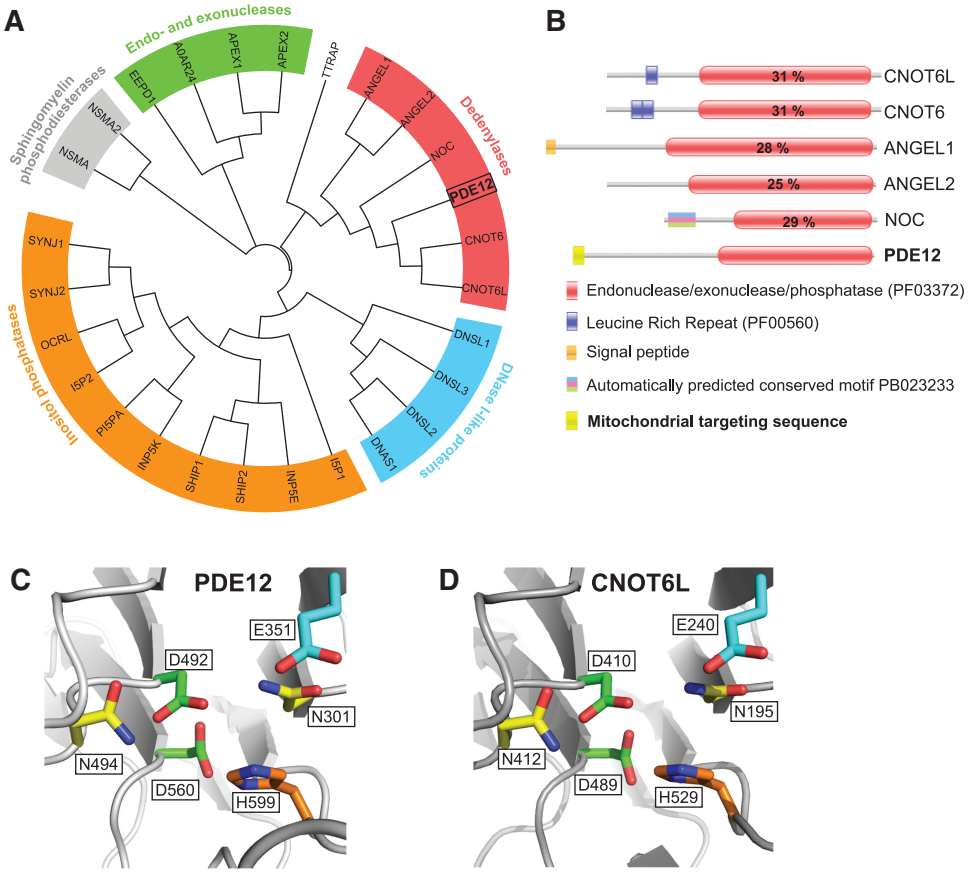

Figure 1. Computational analysis of PDE12. (**A**) The unrooted classification tree of human EEP proteins. The sequences of the catalytic domain of all human proteins of the EEP family (PF03372) were extracted from the Pfam database (see Supplementary Table S1 for details) and aligned using ClustalW2. Five major subgroups identified are indicated on the tree: inositol phosphatases (orange), Sphingomyelin phosphodiesterases (grey), Endo- and exonucleases (green), DNase I-like proteins (blue) and Deadenylases (red). (**B**) Domain architecture of confirmed and putative human deadenylases of the EEP family. Functional domains of human proteins of the 'Deadenylases' subgroup identified in (A) are schematically represented. The position of the EEP domain is represented in each protein by a red box containing the percentage of identity between this domain and that of PDE12. (**C** and **D**) Comparison of the active site structure of PDE12 and other EEP deadenylases. The active site structural motif of PDE12 (C) predicted based on the known crystal structure of the homologous EEP deadenylase CNOT6L (D) using the 3D-Jury algorithm (42) was modelled using the MODELLER 9v1 software (43).

S2B) and their identities were confirmed by mass spectrometry (data not shown).

First, we compared the hydrolytic activity of PDE12 and the E351A mutant using 25 nt-long, homopolymeric RNA (A_{25}) or DNA (dA_{25}) substrates, labelled at their 5′-ends. We observed a time-dependent degradation of the RNA with wild-type, but not E351A mutant, PDE12; neither protein had any effect on DNA (Figure 3A). The degradation of the 5′-end-labelled A_{25} substrate resulted in a progressive and sequential appearance of RNA fragments of lower molecular mass suggesting that the enzyme hydrolyses RNA in the 3′→5′ direction. The addition of a phosphate group at the 3′-end of RNA (substrate A_{25}pCp) completely inhibited RNA degradation, whereas the analogous RNA substrate with a 3′-hydroxyl group (A_{25}pC-OH) was efficiently degraded by the wild-type enzyme (Figure 3A). These results suggest that PDE12 displays specificity for RNA 3′-ends containing a free hydroxyl group, and does not possess 5′→3′ exoribonucleolytic or endoribonucleolytic activity.

Next, we studied the specificity of PDE12 by comparing the time-dependent hydrolytic activity of PDE12 on 25 nt-long homopolymeric RNA substrates i.e. A_{25}, C_{25}, G_{25} or U_{25} (Figure 3B). PDE12 preferred A_{25} and U_{25} as substrates, whereas C_{25} and in particular G_{25} were poorly degraded. The specificity of PDE12 towards poly(A) tails was further characterized on RNA substrates containing: (i) a 111 nt-long 3′-portion of the ND1 human mitochondrial gene (3′ND1) or (ii) the same 3′-portion of ND1 containing a 50 nt poly(A) tail (3′ND1-A_{50}). Analogous substrates containing a 111 nt-long 3′-portion of the CO2 human mitochondrial gene (3′CO2 and 3′CO2-A_{50}, respectively) were also tested. Incubation of recombinant PDE12, but not the E351A mutant, with the polyadenylated substrates (3′ND1-A_{50} or 3′CO2-A_{50}) for 30 min resulted in a size change consistent with the removal of the poly(A) tail (Figure 3C, compare lanes 4 and 5 or 10 and 11). Of note, the enzyme trimmed both substrates ~6–8 nt beyond the poly(A) tail into the body of the message (Figure 3C, compare lanes 1 and 5 or lanes 7 and 11). Incubation of the enzyme with the poly(A)-less substrates (3′ND1 or 3′CO2) resulted in shortening of the message only by ~6–8 nt (Figure 3C, compare lanes 1 and 2 or lanes 7 and 8). Taken together, our results (Figure 3)

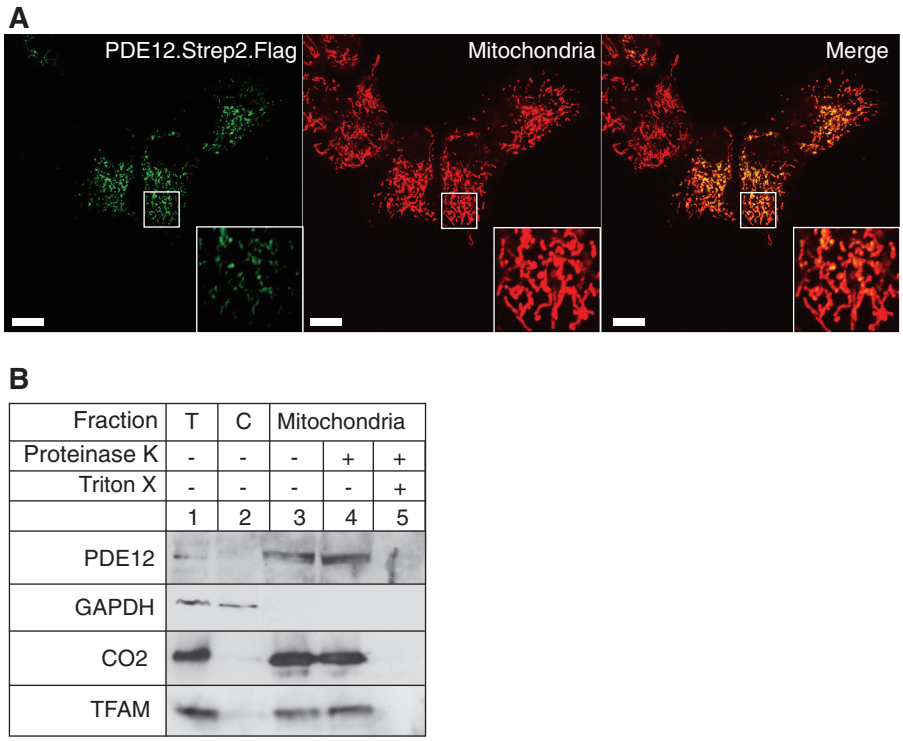

Figure 2. Mitochondrial localization of PDE12. (**A**) The intra-cellular localization of PDE12 by immunofluorescence. The cDNA encoding the Strep2- and Flag-tagged variant of PDE12 was transiently transfected into HOS cells, the protein product was detected by anti-Flag antibody and visualized by secondary antibodies conjugated with FITC (green). Mitochondria were stained with MitoTracker Red CMXRos (red). Co-localization of the green and red signal appears yellow on digitally overlaid images (Merge). (**B**) Location of PDE12 in subcellular fractions. The HOS cells were fractionated into cytosol (C, lane 2) and mitochondria (lanes 3–5) as described 'Material and Methods' section. The mitochondrial fraction was treated with 25 μg/ml proteinase K in the absence (lane 4) or presence of 1% Triton X-100 (lane 5). 'T' denotes the total cell lysate. The protein fractions were analysed by western blotting using antibodies to endogenous PDE12. The location of PDE12 was compared with that of the following marker proteins: TFAM (mitochondrial matrix), CO2 (mitochondrial inner membrane) and GAPDH (cytosol).

indicate that PDE12 can operate as an RNase with specificity for poly(A) tails.

PDE12 transgene expression alters the length of RNA poly(A) tails in mitochondria

Based on the *in vitro* data (Figure 3), a high dose of PDE12 in mitochondria is predicted to shorten poly(A) tails. In order to determine the effect of PDE12 on RNA poly(A) tail length of mitochondrial transcripts, recombinant PDE12 or the E351A catalytic mutant was expressed in HEK293T cells. Both proteins were equally stable in human mitochondria (Figure 4A). In order to map the exact changes in mt-RNA species, total RNA was isolated parental HEK293T cells. The length and sequence of mitochondrial transcripts ND1 and CO2 were analysed after PCR amplification, circularization, reverse transcription and cloning (cRT–PCR). All mitochondrial transcripts analyzed preserved the normal 5′-end, but in approximately half of the CO2 transcripts the length of the poly(A) tail was reduced to 40 adenines or less (48 and 54% for 2 and 4 days of PDE12 overexpression, respectively); all of the ND1 transcripts had poly(A) tails shorter than 40 adenines after 2 or 4 days of PDE12 overexpression (Figure 4B and Supplementary Table S2). In ~8 and 41% of the CO2 and ND1 transcripts, respectively, the poly(A) tail was lost completely 4 days after PDE12 induction. Similarly to the data obtained *in vitro* (Figure 3C), RNA truncation of the ND1 and CO2 transcripts by PDE12 did not stop at the beginning of the poly(A) tract, but continued for up to 8 nt, into the 3′-termini of the transcripts (Supplementary Table S2). Some of the truncated ND1 transcripts were re-adenylated (Supplementary Table S2). Mitochondrial transcripts of cells overexpressing the E351A catalytic mutant were indistinguishable from those of control cells (Figure 4B). These data indicate that PDE12 can degrade poly(A) tails in human mitochondria.

Removal of poly(A) tails by PDE12 has different effects on the stability of the various mitochondrial transcripts

Because there is currently no consensus as to the role of poly(A) tails in the regulation of mitochondrial transcript stability, we studied the effects of elevated mitochondrial PDE12 expression (deadenylase activity) on the steady-state levels of all 11 mt-mRNAs by northern blot analysis. Induction of expression of the PDE12 transgene resulted in a size reduction of mt-mRNAs consistent with the removal of the poly(A) from the mitochondrial transcripts (Figure 4C). Deadenylation had transcript-specific effects on the stability of individual mt-RNAs. After 4

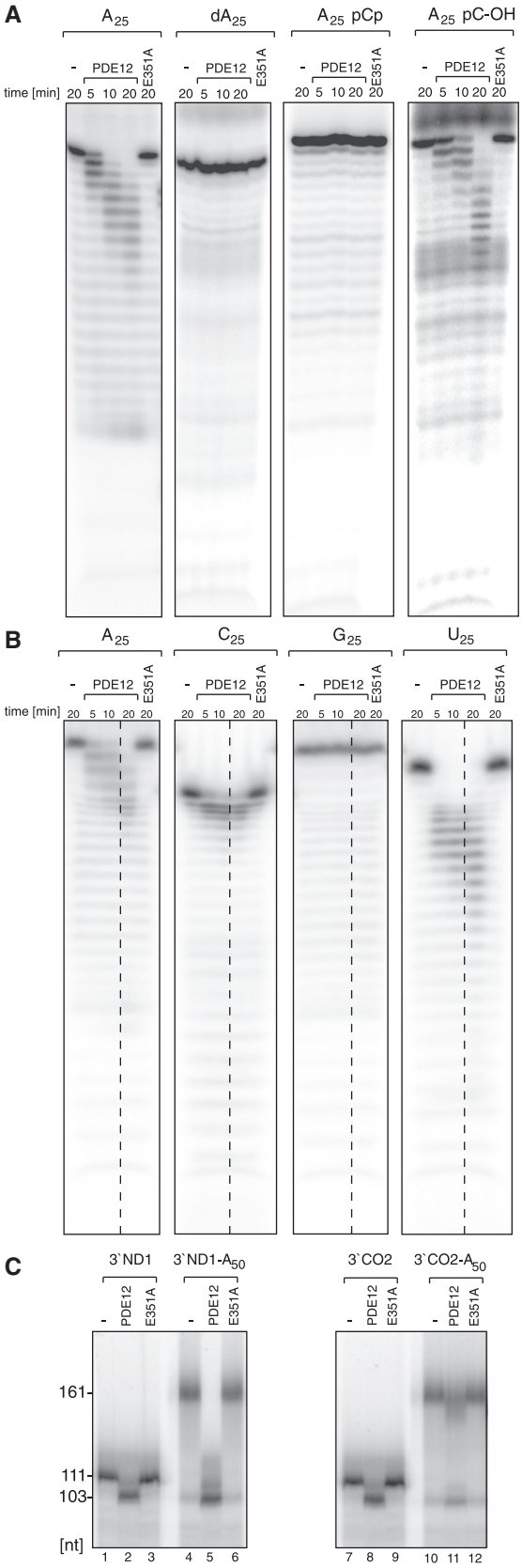

Figure 3. Enzymatic activity of PDE12. (**A**) 3′→5′ exoribonucleolytic activity of PDE12. 8.5 pmoles of PDE12.Strep2.Flag or the E351A catalytic mutant purified from human mitochondria were incubated with 5 pmols of radioactively labelled 25 nt-long homopolymeric adenosine RNA (A_{25}), 25 nt-long homopolymeric adenosine DNA (dA_{25}), 25 nt-long homopolymeric adenosine RNA labelled on the 3′-end with pCp (A_{25}pCp) or 25 nt-long homopolymeric adenosine RNA with cytosine ribonucleotide at the 3′-end (A_{25}pC-OH) for the indicated time. The products were separated on a 10% urea polyacrylamide gel and subjected to autoradiography. (**B**) Sequence specificity of PDE12. 8.5 pmoles of PDE12.Strep2.Flag or the E351A catalytic mutant were incubated with 5 pmoles of radioactively labelled 25 nt-long homopolymeric RNAs consisting of adenine (A_{25}), cytosine (C_{25}), guanine (G_{25}) or uridine (U_{25}) nucleotides for the indicated time. The products were separated on a 10% urea polyacrylamide gel and subjected to autoradiography. (**C**) Deadenylase activity of PDE12 on synthetic mt-RNA substrates. About 8.5 pmols of PDE12.Strep2.Flag or the E351A catalytic mutant were incubated with synthetic transcripts produced by run-off T7 transcription in the presence of radioactive UTP. The following RNAs were tested: 111 nt-long 3′-region of the ND1 ORF (3′ND1, lanes 1–3), 111 nt-long 3′-part of the ND1 ORF containing a 50 nt poly(A) tail (3′ND1-A_{50}, lanes 4–6), 111-nt long 3′-part of the CO2 ORF (3′CO2, lanes 7–9) or 111 nt-long 3′-part of the CO2 ORF containing a 50-nt poly(A) tail (3′CO2-A_{50}, lanes 10–12). The products were separated on a 5% urea polyacrylamide gel and subjected to autoradiography.

days of PDE12 induction, the steady-state levels of ND1 and ND2 mRNAs had doubled, ND3 and CytB mRNAs were one-third higher, whereas the levels of CO1 and CO2 had halved, compared to those of uninduced cells (Figure 4D). There was little change in the steady-state levels of the remaining mt-RNAs: 12 S-rRNA, 16 S-rRNA, ND4, ND5, ND6, CO3 and ATP6/8 mRNAs were within 15% of the starting level, after 4 days of PDE12 induction (Figure 4D). Overexpression of the E351A catalytic mutant did not affect the steady-state level of mt-RNAs (data not shown) consistent with the retention of poly(A) tails (Figure 4B). Although PDE12 has no detectable deoxyribonuclease activity (Figure 3A), it might perturb mtDNA metabolism in some way. However, mtDNA copy number was unchanged in cells expressing PDE12 (Figure 4E).

Elevated levels of PDE12 compromise OXPHOS function

Mitochondrial ATP production and OXPHOS were analysed in cells-expressing PDE12, or the E351A mutant, to investigate the consequences of the increased deadenylase activity on mitochondrial function. Induction of PDE12, but not E351A, resulted in greater acidification of growth media (Supplementary Figure S3), suggesting that elevated expression of PDE12 results in increased dependence on glycolytic as oppose to mitochondrial ATP production. Furthermore, PDE12 transgene expressing cells had a reduced growth rate when cultured in medium containing 25 mM glucose (generation times: PDE12 = 1.42 ± 0.06, HEK293T = 1.27 ± 0.03 and E351A = 1.30 ± 0.03 days) and the growth impairment was accentuated when the cells' reliance on mitochondrial ATP production was increased by culturing them in medium containing galactose as the sole carbon source (generation times: PDE12 = 2.17 ± 0.13, HEK293T = 1.51 ± 0.04 and E351A = 1.48 ± 0.03 days) (Figure 5A). Overexpression of PDE12 for 4 days also resulted in a 35% decrease in mitochondrial

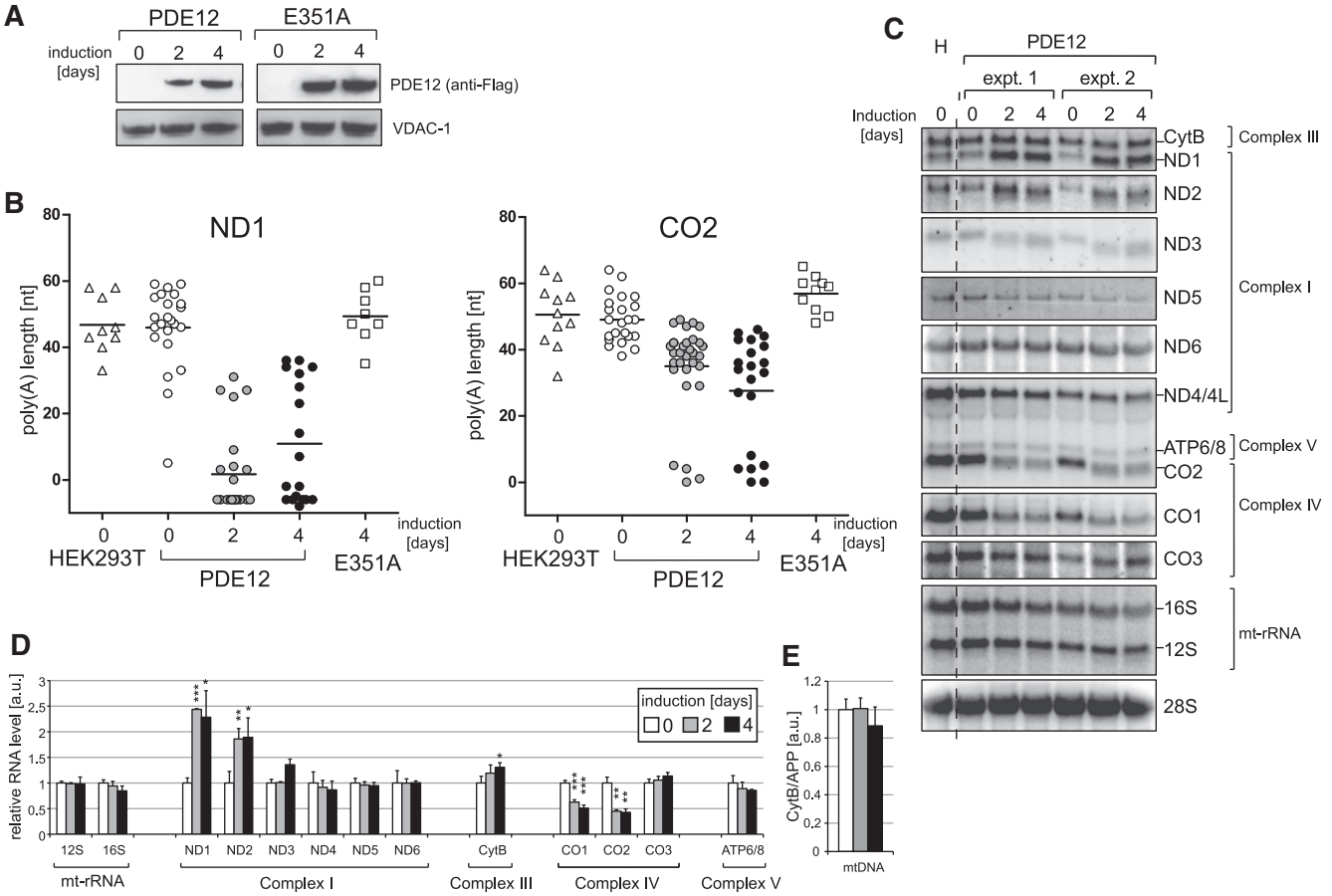

Figure 4. Mitochondrial transcripts in cells overexpressing PDE12. (**A**) Inducible expression of PDE12 and the E351A catalytic mutant in HEK293T cells. Western blot illustrating a time course of expression of PDE12.Strep2.Flag or the E351A mutant induced with 50 ng/ml doxycycline. The PDE12 protein was detected using anti-Flag antibody; anti-VDAC-1 antibodies were used as a mitochondrial loading control. (**B**) Analysis of the poly(A) tail length of mitochondrial transcripts upon PDE12 induction. Mitochondrial ND1 or CO2 mRNAs were analysed by cRT–PCR and sequencing as described in 'Materials and Methods' section. Each data point represents a single clone analysed for the HEK293T parental cells (triangle), wild-type PDE12 (circle) and the E351A mutant (square). The length of poly(A) extensions are given on the *Y*-axis (note that the values below zero indicate transcripts that were truncated beyond the processing/polyadenylation site). Doxycycline induction times are given on the *X*-axis. The horizontal lines represent average lengths of poly(A) tails. (**C**) Northern blots of mitochondrial transcripts upon overexpression of PDE12. Total RNA from parental HEK293T cells (H), uninduced cells (0 days) and cells expressing PDE12 for 2 or 4 days (induced with 50 ng/ml doxycycline) from two independent experiments ('expt. 1′ and 'expt. 2′) were analysed by northern blots using probes specific for all mitochondrial transcripts. Nuclear-encoded 28 S rRNA was used as a loading control. (**D**) Quantification of steady-state levels of mitochondrial transcripts in cells overexpressing PDE12. The values of the relative RNA levels (mt-RNA/28 S rRNA) were obtained by quantifying PhosphorImager scans of northern blots using ImageQuant software and normalized for the values obtained from uninduced cells. $*P < 0.05$, $**P < 0.01$, $***P < 0.001$; $n = 3$, Error bars = 1 SD. (**E**) mtDNA copy number in cells overexpressing PDE12. Comparative Q-PCR of the mitochondrial CytB gene and single copy nuclear gene (APP) was used with total DNA isolated from cells overexpressing PDE12 for the indicated time. $*P < 0.05$, $**P < 0.01$, $***P < 0.001$; $n = 3$, Error bars = 1 SD.

membrane potential (Figure 5B). Finally, we analyzed steady-state levels of respiratory chain subunits, as OXPHOS dysfunction is usually associated with aberrant assembly or instability of mitochondrial respiratory complexes. PDE12 overexpression for 4 or 6 days markedly reduced the abundance of components of complex I and subunits of complex IV (Figure 5C). The observed perturbations in the respiratory complexes in PDE12 overexpressing cells were additionally reflected by cellular oxygen consumption rates (OCR) that were reduced by ~50% of the level of controls (Figure 5D). The above results suggest that overexpression of PDE12 causes a severe defect in oxidative metabolism.

PDE12 transgene overexpression inhibits mitochondrial translation and alters mitoribosomal profile

In order to determine whether the OXPHOS defect in cells overexpressing PDE12 is a consequence of impaired mitochondrial protein synthesis, we labelled the *de novo* synthesized mitochondrially encoded subunits of the electron transport chain with radioactive methionine. After the inhibition of cytosolic translation, the incorporation of ^{35}S-Met into mitochondrial proteins was analysed over a time course of 4 days in HEK293T cells overexpressing PDE12 or the E351A catalytic mutant (Figure 6A). Translation of all mitochondrially encoded respiratory chain subunits was compromised upon the induction of PDE12 overexpression and the incorporation

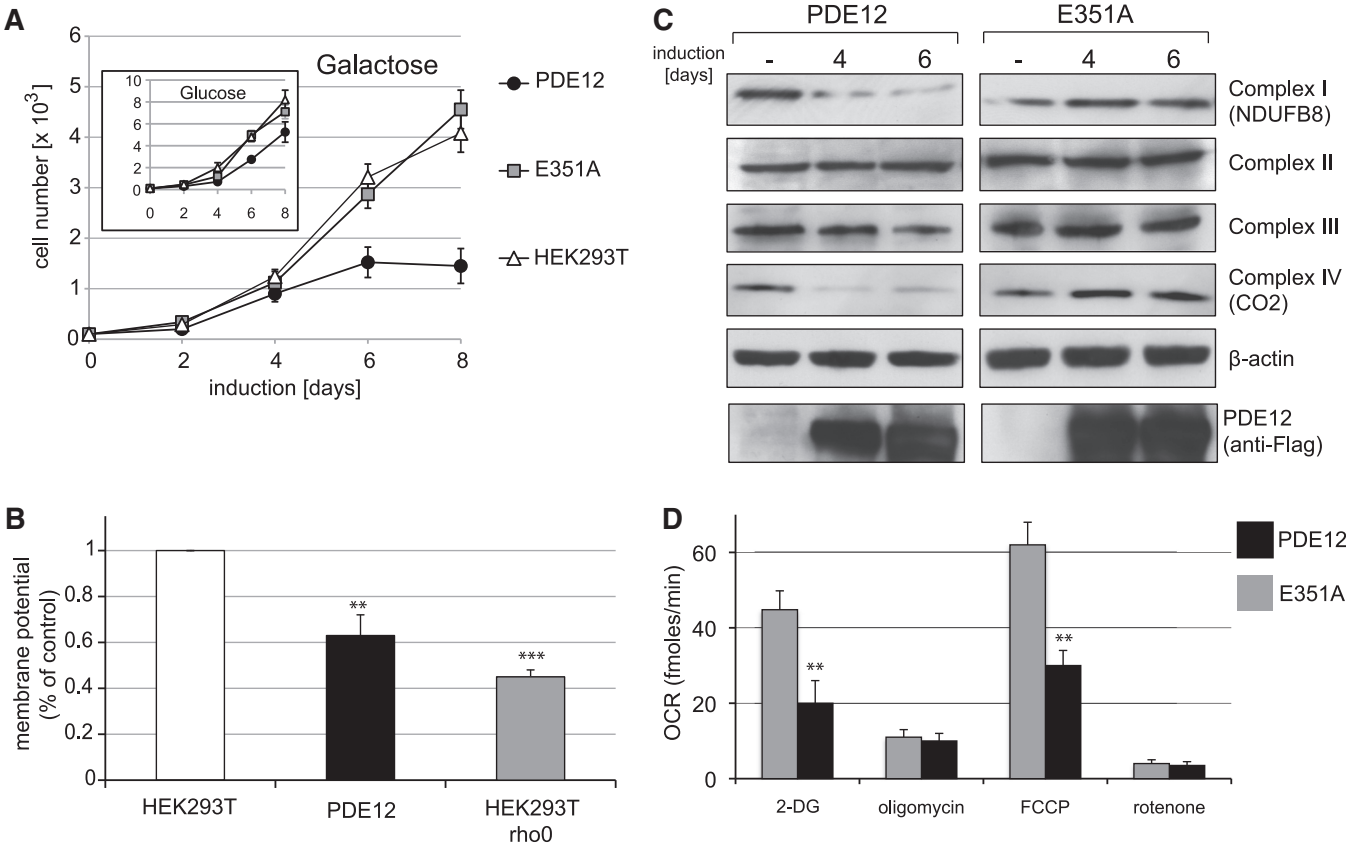

Figure 5. Respiratory chain function upon PDE12 overexpression. (**A**) Growth of cells overexpressing PDE12 on galactose and glucose media. Growth curves of parental HEK293 cells or transfectants-expressing PDE12 or the E351A mutant in galactose or glucose (inset) media and induced for the indicated time. (**B**) Mitochondrial membrane potential in cells overexpressing PDE12. Mitochondrial membrane potential was assessed by a quantitative FACS analysis of TMRE intensity. Twenty thousand cells stained with TMRE were analysed for each sample. The percentages of TMRE intensity were normalized to that of HEK293T cells (= 100%). The mtDNA-less HEK293T cells were used as a negative control. $^{**}P < 0.01$, $^{***}P < 0.001$; two-tailed Student's *t*-test; $n = 3$, Error bars = 1 SD. (**C**) Steady-state level of the OXPHOS subunits in cells overexpressing PDE12. Steady-state protein level of subunits of respiratory chain complexes in uninduced control cells or cells overexpressing PDE12 or its catalytic mutant (E351A) for the indicated time were analysed by western blot. β-Actin was used as a loading control. (**D**) OCR in cells overexpressing PDE12. OCR measured in an extracellular flux Seahorse instrument in a quadruplicate population of control uninduced or cells overexpressing PDE12 or its catalytic mutant (E351A) for 4 days. The wells containing cells were sequentially injected with 20 mM 2-DG to inhibit glycolysis, 100 nM oligomycin to inhibit ATP synthase, 1 μM FCCP to uncouple the respiratory chain and 200 nM rotenone to inhibit complex I.** $P < 0.01$; two-tailed Student's *t*-test; $n = 3$, Error bars = 1 SD.

of ^{35}S-Met was ~15% of those in uninduced cells (Figure 6B). Overexpression of the E351A mutant did not have any appreciable effect upon mitochondrial protein synthesis (Figure 6B). Next, we carried out gradient sedimentation analyses of cell extracts from cells overexpressing PDE12 for 4 days and control cells in order to investigate the integrity of the mitochondrial ribosome (Figure 6C). In this method, we detected the 28 S (small) and 39 S (large) subunits by western blotting of gradient fractions. We used DAP3/MRPS29 as a marker for the 28 S ribosomal subunit and MRPL3 as a marker for the 39 S subunit. The analyses of sedimentation of mitoribosomal subunits upon overexpression of PDE12 revealed: (i) deficiency of assembled 28 S mitoribosomal subunits as compared to the control and (ii) anomalous sedimentation of the 39 S subunits that was shifted towards slower migrating species (Figure 6C). These changes in mitoribosomes were not due to any alteration in the length of the mitochondrial rRNAs, based on RNase protection assays of 12 S and 16 S rRNA (Supplementary Figure S4A–B). Nor was the steady-state level or length of 7 mt-tRNAs (Ser-UCN, Leu-UUR, Thr, Gln, Pro, Lys and Phe) affected by elevated PDE12 expression (Supplementary Figure S4C–D). However, in the case of tRNASer-AGY the steady-state level of the full-length molecule was ~60% of the control value after 4 days of PDE12 overexpression and a species of lower molecular mass was detected. A similar truncated form of tRNASer-AGY, albeit of much lower abundance, was observed in control cells (Supplementary Figure S4C). Mutant tRNA levels considerably >50% are needed to produce a mitochondrial translation defect (24) and so the observed inhibition of mitochondrial translation is most likely attributable to the shortening of the mt-RNA poly(A) tails, owing to mitochondrial ribosome instability and/or impaired assembly.

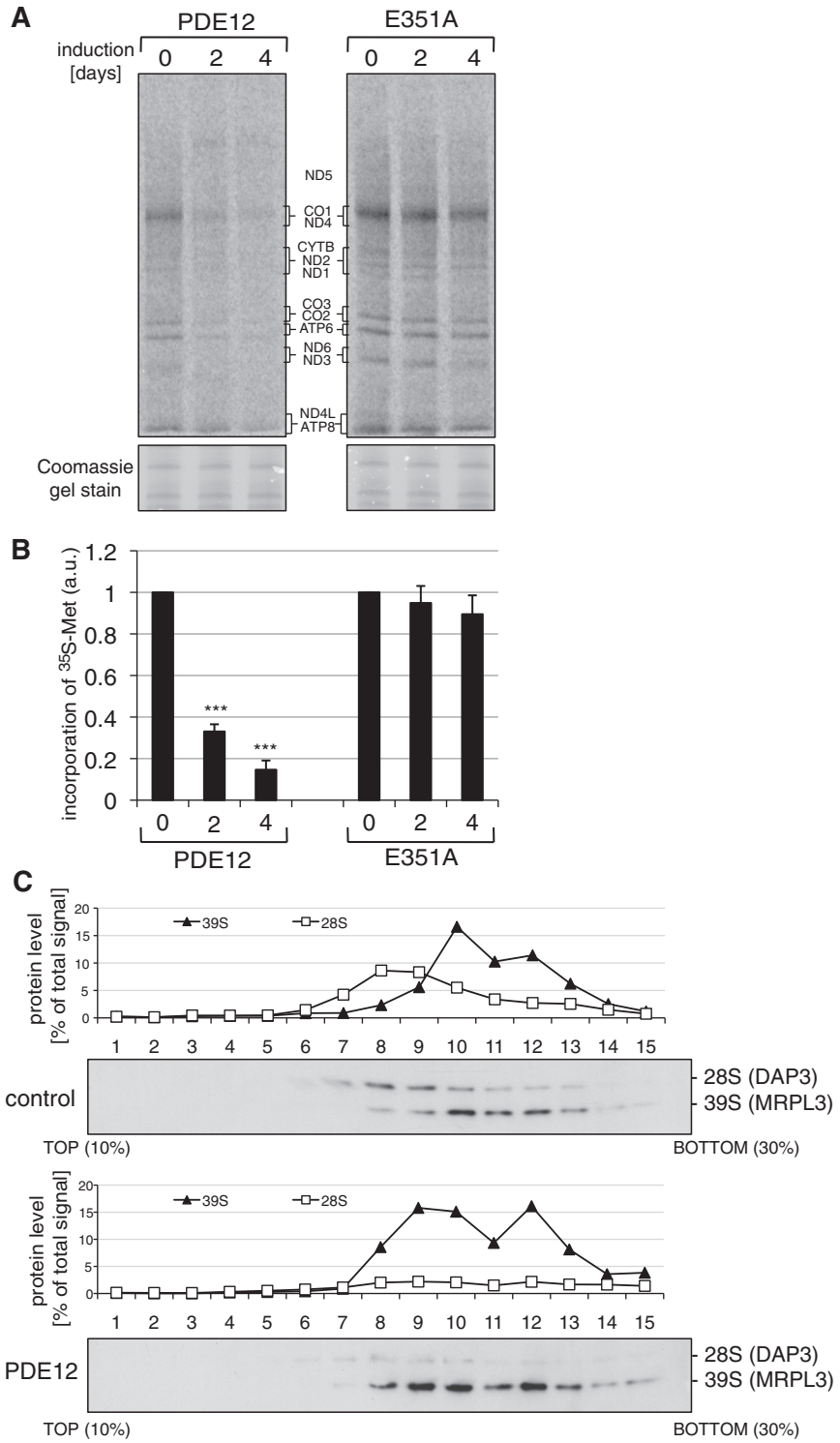

Figure 6. Mitochondrial translation in cells overexpressing PDE12**.** (**A**) Products of mitochondrial translation were labelled with ^{35}S 36methionine for 15 min after expression of PDE12 or the E351A catalytic mutant in HEK293T cells for 2 or 4 days as described in 'Materials and Methods' section. Mitochondrial proteins were separated by a 4–12% gradient SDS–PAGE and visualized by autoradiography. To validate equal protein loading, a small section of the gel was stained with Coomassie. (**B**) Radiolabelled products of mitochondrial translation as in (A) were quantified using ImageQuant software following exposure to a PhosphorImager cassette. ***$P < 0.001$; two-tailed Student's t-test; $n = 4$, Error bars = 1 SD. (**C**) Mitochondrial ribosome profile in cells overexpressing PDE12. Cell lysates of HEK293T cells overexpressing PDE12 for 4 days or control cells were separated on a 10–30% (v:v) isokinetic sucrose gradient. Fractions obtained for control and PDE12 overexpressing cells were analysed by western blot simultaneously with antibodies to MRPL3 (39 S mitoribosomal subunit) and DAP3 (28 S mitoribosomal subunit).

DISCUSSION

In this work, we show that the EEP family protein PDE12 is the human mitochondrial poly(A)-specific exoribonuclease. Previously, it has been suggested that human polynucleotide phosphorylase (PNPase), which has a phosphorolytic 3′→5′ exoribonuclease and a poly(A) polymerase activity, might be responsible for poly(A) removal in mitochondria (14). However, hPNPase has been localized to the mitochondrial inter-membrane space, rather than the matrix where mt-RNA resides, and a role in processing of mitochondrial transcripts has been suggested, most likely by indirect means (15,25). As there is no published data on the presence of other enzymes from the DEDD of EEP family in human mitochondria, therefore, PDE12 is the first recognized human mt-RNA deadenylase.

PDE12 as a mitochondrial deadenylase

In the present study, we show that human PDE12 degrades poly(A) tails *in vitro* and that elevated expression of PDE12 results in shortening of poly(A) tails of certain mt-mRNAs in human cultured cells. The previous classification of PDE12 (2′-PDE) as an EEP-type deadenylase by Goldstrohm and Wickens (16) was circumstantial; PDE12 was reported to cleave phosphodiester bonds in short oligo(A) substrates when the 5′-phosphates of each adenosine are covalently linked between either the 2′- or 3′-hydroxyl positions (19). Until recently, the only suggested biological role of PDE12 has been the degradation of 2′–5′-linked oligo(A) in the RNase L innate immune response system and its cellular localization had not been studied (19). While our manuscript was in preparation, Poulsen *et al*. (22) reported the mitochondrial localization of PDE12 and confirmed that recombinant PDE12 produced in *Escherichia coli* is capable of degrading 3′–5′-linked RNA. Relatively short RNA substrates were used containing either (i) a 20-residue generic unstructured RNA sequence followed by 10 adenosine or cytosine residues or (ii) an RNA consisting of an 8 bp strong stem–loop structure followed by 10 adenosine residues. Longer incubation of the recombinant enzyme that lacked the predicted MTS with all three RNA substrates resulted in degradation into small fragments of 4–11 nt in size with comparable efficiency for all three substrates (22). In contrast, our studies of the biochemical properties of PDE12 isolated from human mitochondria show that PDE12 efficiently degrades poly(A) and poly(U), whereas poly(C) and poly(G) are not preferred substrates. Thus, PDE12 shares the same preference for poly(A) or poly(U) substrates as cytoplasmic deadenylases, such as PARN (26) and POP2 (27). Furthermore, we found that PDE12 isolated from mitochondria exhibits strong specificity to poly(A) when relatively long substrates containing a fragment of endogenous human mitochondrial sequence (over 100 nt of the 3′-end of ND1 or CO2) and poly(A) tails of 50 nt (close to the physiological length of the tails in mt-mRNAs) were used. The enzyme degraded maximally eight residues beyond the mRNA-poly(A) tail boundary. Eight nucleotides was also the maximum number of bases removed beyond the poly(A) tail of mt-mRNAs isolated from cells overexpressing PDE12. Therefore, human PDE12 has characteristics typical of a number of deadenylases: PARN, CCR4 and CAF1 (23,28). Moreover, as no RNA was truncated beyond the −8 position, PDE12 is not likely to be responsible for a general mt-RNA decay, as previously suggested (22). The discrepancy between the activity of PDE12 on RNA reported by Poulsen *et al*. (22) and in the current study could be owing to: (i) the molar ratio of the enzyme to RNA (100:1 and 1.7:1, respectively); (ii) the source of the purified enzyme (*E. coli* and human mitochondria, respectively); or (iii) the use of RNA substrates containing arbitrary rather then natural mitochondrial sequences (see above).

The poly(U)-degrading property of PDE12 (Figure 3B) could be of biological significance, as the presence of poly(U) tails in human mt-RNA has been reported recently (15,29,30). Interestingly, the polyuridinylated RNA identified in these cases contained unprocessed upstream or downstream tRNA genes in addition to a protein-coding region, and therefore might represent products of improper processing of the polycistronic precursor. This suggests that poly(U) tails play a role in the degradation of mt-RNA, and that PDE12 might contribute to this process.

PDE12 has been suggested to play a role in 2′-5′-adenylate catabolism in the RNaseL innate immune response system. As all components of this pathway are localized in the cytosol, it is difficult to explain the previously postulated role of PDE12 in the context of its mitochondrial localization. It is possible, however, that an alternatively localized form of the enzyme exists, which is involved in the regulation of the RNaseL pathway, as suggested previously (22). Of note, degradation of both 2′-5′- and 3′-5′-linked oligoriboadenylates has been reported previously for other poly(A)-specific exoribonucleases (31,32) and might therefore represent a common property of this class of enzyme.

Mitochondrial poly(A) tails and RNA stability

Polyadenylation plays an important role in regulating mRNA stability in many systems [see 'Introduction' section and ref. (7)]. The role of mitochondrial poly(A) tails in controlling the stability of mRNA has been debated. Different approaches have been undertaken to address this issue in human mitochondria: (i) prevention of the synthesis of mitochondrial poly(A) by depleting hmtPAP levels with siRNA (3,4,10) or (ii) trimming poly(A) tails by targeting the cytosolic poly(A)-specific nuclease PARN to mitochondria (12). Independent studies of hmtPAP gene silencing reached quite different conclusions as shortening of poly(A) tails did not affect the stability of the analysed mitochondrial transcripts (ND3, CO3 and ATP6/8) in one study (3), whereas others found that the abundance of several mitochondrial transcripts decreased in response to hmtPAP siRNA (4,10). It should be stressed, however, that siRNA-induced downregulation of hmtPAP might not have been complete and also the existence of a second polyadenylating enzyme has been postulated (33,34) that

would additionally complicate the interpretation of the results of the downregulation of hmtPAP by siRNA. On the other hand, mitochondrial targeting of PARN completely removed the 3′-poly(A) extensions of mt-RNAs (12). This had a variable effect on mt-mRNA steady-state levels, increasing some (ND1, ND2 and ND5) and decreasing others (CO1, CO2 and ATP6/8), whilst still others were little changed (ND4/4 L and ND3). Deadenylation of mitochondrial transcripts as a result of overexpression of PDE12 had a very similar effect on the steady-state levels of the above transcripts (Figure 4D). Thus, in both studies removing poly(A) tails from mt-mRNAs destabilized CO1 and CO2, whereas poly(A) addition promotes turnover of ND1 and ND2 mRNAs in human mitochondria, as previously proposed (15,33). Therefore, there is no universal role of mitochondrial poly(A) tails in regulation of the RNA stability, and two classes of poly(A) tails might exist in mitochondria that have opposite regulatory functions i.e. either stabilization or destabilization. If stable and degradation inducing poly(A) tails exist in mitochondria, how do animal mitochondria differentiate between them? Our data show that the efficiency of degrading of the poly(A) tails by PDE12 *in vitro* is different for certain transcripts, e.g. PDE12 deadenylates ND1 more efficiently than CO2 *in vitro* (Figure 3C), and in cells (Figure 4B). This might suggest the presence of RNA 3′-end *cis*-regulatory elements that modulate the deadenylating activity of PDE12. Perhaps, the structure of the 3′-end of the CO2 mRNA partially protects the transcript from deadenylation, which is particularly intriguing in light of the fact that the CO2 messenger becomes unstable upon removal of the poly(A) tail. In summary, our data confirm a previous suggestion (6,35) that polyadenylation itself is not sufficient to direct mt-RNA for degradation or to stabilise mitochondrial transcripts and that the regulation of RNA turnover must depend on additional, yet to be identified, factors.

PDE12 as a regulator of mitochondrial translation

Our data show that PDE12 is important for regulating translation efficiency in human mitochondria. The overexpression of PDE12 resulted in decreased translation rates for all mitochondrial proteins (Figure 6) despite the fact that the steady-state levels of the majority of transcripts were not changed or were up-regulated (Figure 4D). There was an ~50% reduction in the steady-state levels of only two transcripts—CO1 and CO2. However, it is unlikely that the down-regulation of these individual transcripts could have caused the general inhibition of mitochondrial translation, as published data indicates that a comparable reduction in the steady-state levels of two or more human mitochondrial transcripts does not lead to a global translational defect affecting all mtDNA-encoded proteins (36). The effect on mitochondrial protein synthesis is likely to result from the removal of poly(A) tails by the exoribonucleolytic activity of PDE12, rather then from a direct interaction of the enzyme with the mitochondrial translation machinery (e.g. ribosomes or translation factors) or from an indirect effect related to a defect in cell growth. This is supported by the lack of co-sedimentation of PDE12 with mitoribosomes in sucrose gradient experiments or the lack of interaction with mitoribosomal proteins in pull-down experiments (data not shown). Also, conditions that increase cells' reliance on mitochondrial ATP production exacerbated the observed growth phenotype (Figure 5A). No alterations were observed in the abundance of components of complex II (containing only nuclearly encoded and cytoplasmically translated subunits) nor other cytoplasmic proteins (β-actin or GAPDH) suggesting a specifically mitochondrial, rather than cytoplasmic, effect in cells overexpressing PDE12. Here, again our findings are concordant with another study in which mt-mRNA poly(A) tails were removed by mitochondrial targeting of the cytosolic deadenylase PARN or coated by mitochondrially targeted human cytosolic poly(A)-binding protein, PABPC1 (12), both of which resulted in marked inhibition of mitochondrial translation.

We excluded the possibility that mitochondrial translation is inhibited as a consequence of the partial degradation of mt-rRNAs by PDE12 causing instability or impeding the assembly of mitoribosomes. This is in agreement with the observation that the 3′-termini of mt-rRNAs normally do not have >1–2 nt adenine nucleotides (3) and therefore might not present good substrates for PDE12 deadenylation. Also, we did not observe a marked change in the steady-state levels of the majority of mt-tRNAs analysed. Only tRNA-SerAGY—the unusual mt-tRNA, which does not fold into cloverleaf structure (37)—was downregulated by ~40% and a shorter species was observed for this mt-tRNA. This change is unlikely to account for the dramatic (almost 90%) translation inhibition observed after PDE12 overexpression. As the truncated product of tRNASer-AGY was also observed in control cells, it might represent a relatively stable decay intermediate, which is more abundant in cells with inhibited mitochondrial translation, rather then a PDE12 degradation product.

Translation is principally controlled at the initiation stage (rather than elongation or termination), allowing for rapid, reversible and spatial regulation of cellular concentrations of proteins. Nuclear-encoded eukaryotic transcripts are polyadenylated by the nuclear polyadenylation machinery. Once the mRNA is transported to the cytoplasm, poly(A) not only stabilize RNA, but also promotes translation initiation. Eukaryotic cytoplasmic initiation factors recognize the 5′-mRNA m^7G cap structure and the 3′-poly(A) tail via poly(A)-binding protein leading to circularization of the mRNA, which is necessary for translation initiation (38). The architecture of the mitochondrial translation initiation machinery resembles the one found in bacteria (8), and both bacterial and mitochondrial mt-mRNAs lack the 5′-end cap structure. However, mature bacterial messengers do not contain poly(A) tails as polyadenylation consistently promotes mRNA degradation in prokaryotes. If, by analogy to *Eukaryota*, mitochondrial poly(A) tails play a role in translation initiation their removal might primarily affect the stability of the 28 S small ribosomal subunit as this subunit binds mRNA prior to assembly of the 55 S mitoribosome (39).

This would be consistent with the results of our analysis of mitoribosomal sedimentation on isokinetic density gradients that shows the steady-state level of the 28 S subunit was notably lower in cells, in which mt-mRNAs were deadenylated by PDE12 overexpression.

The exonucleolytic activity of PDE12 can extend several nucleotides beyond the processing/polyadenylation site (Figures 3C and 4B). This observation brings about an alternative explanation of how polyadenylation could influence mitochondrial translation. For 7 of 13 mitochondrial ORFs (ND1, ND2 ND3, ND4, CytB, CO3 and ATP6) removal of several terminal ribonucleotides (e.g. eight as seen for the ND1 mRNA) would result in truncation of a translation stop codon and at least two protein-coding triplets. This might be sufficient to inhibit translation owing to mitoribosome stalling. Studies of bacterial and eukaryotic systems have identified several mechanisms of regulatory stalling of ribosomes that inhibits protein synthesis (40,41). However, the remaining six mitochondrial transcripts, ND4L, ND5, ND6, CO1, CO2 and ATP8, contain 3′-UTRs prior to poly(A) extension that are long enough to ensure the presence of an entire ORF, even after the removal of 8 nt. Nonetheless, notably lowered steady-state levels of deadenylated mRNAs-encoding CO1, CO2 and ATP6/8 were observed in our experiments (Figure 4C) and have been reported previously by others (4,10,12). Therefore, the deadenylation-mediated inhibition of mitochondrial translation could depend on two simultaneous events: removal of the last 2–3 codons from the 3′-ends causing ribosome stalling and destabilization of mRNAs containing 3′-UTRs.

In summary, our study identifies PDE12 as an RNase that is directly involved in the regulation of mRNA poly(A) tail lengths in mitochondria. Our results also underscore the importance of poly(A) tails in modulation of mitochondrial gene expression and suggest that in addition to being required for completing the termination codon of seven mitochondrial ORFs, they also play a role in mitochondrial protein synthesis.

SUPPLEMENTARY DATA

Supplementary Data are available at NAR Online.

ACKNOWLEDGEMENTS

We would like to thank Ian Holt for stimulating discussions and help with the manuscript. We are also grateful to Marcin Pekalski for his help with the FACS analysis.

FUNDING

This work was supported by the Medical Research Council. Funding for open access charge: MRC.

Conflict of interest statement. None declared.

REFERENCES

1. Anderson,S., Bankier,A.T., Barrell,B.G., de Bruijn,M.H., Coulson,A.R., Drouin,J., Eperon,I.C., Nierlich,D.P., Roe,B.A., Sanger,F. *et al.* (1981) Sequence and organization of the human mitochondrial genome. *Nature*, **290**, 457–465.
2. Montoya,J., Christianson,T., Levens,D., Rabinowitz,M. and Attardi,G. (1982) Identification of initiation sites for heavy-strand and light-strand transcription in human mitochondrial DNA. *Proc. Natl Acad. Sci. USA*, **79**, 7195–7199.
3. Tomecki,R., Dmochowska,A., Gewartowski,K., Dziembowski,A. and Stepien,P.P. (2004) Identification of a novel human nuclear-encoded mitochondrial poly(A) polymerase. *Nucleic Acids Res.*, **32**, 6001–6014.
4. Nagaike,T., Suzuki,T., Katoh,T. and Ueda,T. (2005) Human mitochondrial mRNAs are stabilized with polyadenylation regulated by mitochondria-specific poly(A) polymerase and polynucleotide phosphorylase. *J. Biol. Chem.*, **280**, 19721–19727.
5. Temperley,R.J., Wydro,M., Lightowlers,R.N. and Chrzanowska-Lightowlers,Z.M. (2010) Human mitochondrial mRNAs-like members of all families, similar but different. *Biochim. Biophys. Acta*, **1797**, 1081–1085.
6. Borowski,L.S., Szczesny,R.J., Brzezniak,L.K. and Stepien,P.P. (2010) RNA turnover in human mitochondria: more questions than answers? *Biochim. Biophys. Acta*, **1797**, 1066–1070.
7. Gagliardi,D., Stepien,P.P., Temperley,R.J., Lightowlers,R.N. and Chrzanowska-Lightowlers,Z.M. (2004) Messenger RNA stability in mitochondria: different means to an end. *Trends Genet.*, **20**, 260–267.
8. Rorbach,J., Soleimanpour-Lichaei,R., Lightowlers,R.N. and Chrzanowska-Lightowlers,Z.M. (2007) How do mammalian mitochondria synthesize proteins? *Biochem. Soc. Trans.*, **35**, 1290–1291.
9. Edmonds,M. (2002) A history of poly A sequences: from formation to factors to function. *Prog. Nucleic Acid Res. Mol. Biol.*, **71**, 285–389.
10. Nagao,A., Hino-Shigi,N. and Suzuki,T. (2008) Measuring mRNA decay in human mitochondria. *Methods Enzymol.*, **447**, 489–499.
11. Temperley,R.J., Seneca,S.H., Tonska,K., Bartnik,E., Bindoff,L.A., Lightowlers,R.N. and Chrzanowska-Lightowlers,Z.M. (2003) Investigation of a pathogenic mtDNA microdeletion reveals a translation-dependent deadenylation decay pathway in human mitochondria. *Hum. Mol. Genet.*, **12**, 2341–2348.
12. Wydro,M., Bobrowicz,A., Temperley,R.J., Lightowlers,R.N. and Chrzanowska-Lightowlers,Z.M. (2010) Targeting of the cytosolic poly(A) binding protein PABPC1 to mitochondria causes mitochondrial translation inhibition. *Nucleic Acids Res.*, **38**, 3732–3742.
13. Slomovic,S., Laufer,D., Geiger,D. and Schuster,G. (2005) Polyadenylation and degradation of human mitochondrial RNA: the prokaryotic past leaves its mark. *Mol. Cell. Biol.*, **25**, 6427–6435.
14. Piwowarski,J., Grzechnik,P., Dziembowski,A., Dmochowska,A., Minczuk,M. and Stepien,P.P. (2003) Human polynucleotide phosphorylase, hPNPase, is localized in mitochondria. *J. Mol. Biol.*, **329**, 853–857.
15. Slomovic,S. and Schuster,G. (2008) Stable PNPase RNAi silencing: its effect on the processing and adenylation of human mitochondrial RNA. *RNA*, **14**, 310–323.
16. Goldstrohm,A.C. and Wickens,M. (2008) Multifunctional deadenylase complexes diversify mRNA control. *Nat. Rev. Mol. Cell. Biol.*, **9**, 337–344.
17. Minczuk,M., Kolasinska-Zwierz,P., Murphy,M.P. and Papworth,M.A. (2010) Construction and testing of engineered zinc-finger proteins for sequence-specific modification of mtDNA. *Nat. Protoc.*, **5**, 342–356.
18. Minczuk,M., He,J., Duch,A.M., Ettema,T.J., Chlebowski,A., Dzionek,K., Nijtmans,L.G., Huynen,M.A. and Holt,I.J. (2011) TEFM (c17orf42) is necessary for transcription of human mtDNA. *Nucleic Acids Res.*, **39**, 4284–4299.
19. Kubota,K., Nakahara,K., Ohtsuka,T., Yoshida,S., Kawaguchi,J., Fujita,Y., Ozeki,Y., Hara,A., Yoshimura,C., Furukawa,H. *et al.* (2004) Identification of 2′-phosphodiesterase, which plays a role in

the 2-5A system regulated by interferon. *J. Biol. Chem.*, **279**, 37832–37841.
20. Wang,H., Morita,M., Yang,X., Suzuki,T., Yang,W., Wang,J., Ito,K., Wang,Q., Zhao,C., Bartlam,M. *et al.* (2010) Crystal structure of the human CNOT6L nuclease domain reveals strict poly(A) substrate specificity. *EMBO J.*, **29**, 2566–2576.
21. Pagliarini,D.J., Calvo,S.E., Chang,B., Sheth,S.A., Vafai,S.B., Ong,S.E., Walford,G.A., Sugiana,C., Boneh,A., Chen,W.K. *et al.* (2008) A mitochondrial protein compendium elucidates complex I disease biology. *Cell*, **134**, 112–123.
22. Poulsen,J.B., Andersen,K.R., Kjaer,K.H., Durand,F., Faou,P., Vestergaard,A.L., Talbo,G.H., Hoogenraad,N., Brodersen,D.E., Justesen,J. *et al.* (2011) Human 2′-phosphodiesterase localizes to the mitochondrial matrix with a putative function in mitochondrial RNA turnover. *Nucleic Acids Res.*, **39**, 3754–3770.
23. Baggs,J.E. and Green,C.B. (2003) Nocturnin, a deadenylase in Xenopus laevis retina: a mechanism for posttranscriptional control of circadian-related mRNA. *Curr. Biol.*, **13**, 189–198.
24. Rossignol,R., Faustin,B., Rocher,C., Malgat,M., Mazat,J.P. and Letellier,T. (2003) Mitochondrial threshold effects. *Biochem. J.*, **370**, 751–762.
25. Wang,G., Chen,H.W., Oktay,Y., Zhang,J., Allen,E.L., Smith,G.M., Fan,K.C., Hong,J.S., French,S.W., McCaffery,J.M. *et al.* (2010) PNPASE regulates RNA import into mitochondria. *Cell*, **142**, 456–467.
26. Henriksson,N., Nilsson,P., Wu,M., Song,H. and Virtanen,A. (2010) Recognition of adenosine residues by the active site of poly(A)-specific ribonuclease. *J. Biol. Chem.*, **285**, 163–170.
27. Andersen,K.R., Jonstrup,A.T., Van,L.B. and Brodersen,D.E. (2009) The activity and selectivity of fission yeast Pop2p are affected by a high affinity for Zn2+ and Mn2+ in the active site. *RNA*, **15**, 850–861.
28. Cooke,A., Prigge,A. and Wickens,M. (2010) Translational repression by deadenylases. *J. Biol. Chem.*, **285**, 28506–28513.
29. Brown,T.A., Tkachuk,A.N. and Clayton,D.A. (2008) Native R-loops persist throughout the mouse mitochondrial DNA genome. *J. Biol. Chem.*, **283**, 36743–36751.
30. Szczesny,R.J., Borowski,L.S., Brzezniak,L.K., Dmochowska,A., Gewartowski,K., Bartnik,E. and Stepien,P.P. (2010) Human mitochondrial RNA turnover caught in flagranti: involvement of hSuv3p helicase in RNA surveillance. *Nucleic Acids Res.*, **38**, 279–298.
31. Schroder,H.C., Zahn,R.K., Dose,K. and Muller,W.E. (1980) Purification and characterization of a poly(A)-specific exoribonuclease from calf thymus. *J. Biol. Chem.*, **255**, 4535–4538.
32. Muller,W.E., Schroder,H.C., Zahn,R.K. and Dose,K. (1980) Degradation of 2′-5′-linked oligoriboadenylates by 3′-exoribonuclease and 5′-nucleotidase from calf thymus. *Hoppe Seylers Z. Physiol. Chem.*, **361**, 469–472.
33. Schuster,G. and Stern,D. (2009) RNA polyadenylation and decay in mitochondria and chloroplasts. *Prog. Mol. Biol. Transl. Sci.*, **85**, 393–422.
34. Crosby,A.H., Patel,H., Chioza,B.A., Proukakis,C., Gurtz,K., Patton,M.A., Sharifi,R., Harlalka,G., Simpson,M.A., Dick,K. *et al.* (2010) Defective mitochondrial mRNA maturation is associated with spastic ataxia. *Am. J. Hum. Genet.*, **87**, 655–660.
35. Bobrowicz,A.J., Lightowlers,R.N. and Chrzanowska-Lightowlers,Z. (2008) Polyadenylation and degradation of mRNA in mammalian mitochondria: a missing link? *Biochem. Soc. Trans.*, **36**, 517–519.
36. Sasarman,F., Brunel-Guitton,C., Antonicka,H., Wai,T. and Shoubridge,E.A. (2010) LRPPRC and SLIRP interact in a ribonucleoprotein complex that regulates posttranscriptional gene expression in mitochondria. *Mol. Biol. Cell*, **21**, 1315–1323.
37. Steinberg,S. and Cedergren,R. (1994) Structural compensation in atypical mitochondrial tRNAs. *Nat. Struct. Biol.*, **1**, 507–510.
38. Jackson,R.J., Hellen,C.U. and Pestova,T.V. (2010) The mechanism of eukaryotic translation initiation and principles of its regulation. *Nat. Rev. Mol. Cell. Biol.*, **11**, 113–127.
39. Christian,B.E. and Spremulli,L.L. (2010) Preferential selection of the 5′-terminal start codon on leaderless mRNAs by mammalian mitochondrial ribosomes. *J. Biol. Chem.*, **285**, 28379–28386.
40. Cruz-Vera,L.R., Sachs,M.S., Squires,C.L. and Yanofsky,C. (2011) Nascent polypeptide sequences that influence ribosome function. *Curr. Opin. Microbiol.*, **14**, 160–166.
41. Zahn,K. (1996) Overexpression of an mRNA dependent on rare codons inhibits protein synthesis and cell growth. *J. Bacteriol.*, **178**, 2926–2933.
42. Ginalski,K., Elofsson,A., Fischer,D. and Rychlewski,L. (2003) 3D-Jury: a simple approach to improve protein structure predictions. *Bioinformatics*, **19**, 1015–1018.
43. Eswar,N., Webb,B., Marti-Renom,M.A., Madhusudhan,M.S., Eramian,D., Shen,M.Y., Pieper,U. and Sali,A. (2006) Comparative protein structure modelling using Modeller. *Curr. Protoc. Bioinformatics*, Chapter 5, Unit 5 6.